# A Range Sidelobe Suppression Technique based on Adaptive Spectral Shaping for LFM Waveforms

Van Khanh Nguyen and Mike D. E. Turley
National Security and ISR Division, Defence Science and Technology
P.O. Box 1500, Edinburgh 5111, AUSTRALIA
Van.Nguyen@dst.defence.gov.au; Mike.Turley@dst.defence.gov.au

***Abstract*—This paper considers the problem of adaptively controlling range sidelobes of target returns for radar systems employing linear frequency modulated (LFM) waveforms. Conventional pulse compression method uses a fixed window to shape the spectral response of a reference waveform to control the range sidelobes of all radar returns. This non-adaptive approach needs to apply a severe spectral window with a peak to sidelobe ratio (PSR) that exceeds the signal to noise ratio (SNR) of the strongest return to ensure successful detection of weak targets in the presence of strong radar returns. This leads to unnecessary processing loss for weak targets. In this paper we propose a new range sidelobe suppression technique that adaptively shapes target spectral response to reduce the processing loss, in particular for weak targets, thereby improving detection sensitivity of the radar systems. It is significantly less complex than many existing range sidelobe suppression techniques. We verify the performance improvement of the proposed adaptive technique over the conventional non-adaptive technique using both simulated and real data.**

## I. Introduction

Detection of weak target returns in the presence of other strong scatterer echoes is an important problem in many radar applications. As an example, received signals in high frequency (HF) skywave radar systems often contain echoes from meteor trails, ground and sea scatterers that are thousand times stronger than returns from targets of interest. In order to successfully detect the weak targets, range and Doppler sidelobes of the strong echoes need to be suppressed. In this paper, we focus on suppressing the range sidelobes.

Pulse compression is a common technique of achieving range resolution for long radar pulses. A standard approach in pulse compression is to correlate the received signal with a reference waveform. For a point scatterer in white Gaussian noise, it is well-known that correlating the received signal with a delayed copy of the transmitted waveform, i.e. a matched filter (MF), maximises the output signal-to-noise ratio (SNR). Unfortunately, the MF output has a low peak to sidelobe ratio (PSR). When the received signal contains both strong and weak echoes, the presence of weak targets can be masked by the range sidelobes of a sufficiently stronger echo if they are not suppressed adequately. To achieve range sidelobe suppression for radar systems with LFM waveforms, a spectral window is often utilised to shape the spectral response of the reference waveform, leading to a mismatched filter [2], [3]. The penalty for this mismatch is a reduction in the target output SNR, which is subsequently referred to as processing loss. The magnitude of this loss is dependent on the spectral window being used. A severely tapered window that possesses high PSR, hence providing greater range sidelobe suppression capability, will have greater processing loss [4]. To account for range sidelobes of the strongest echo, the conventional pulse compression approach normally uses windows with a PSR that exceeds the SNR of the strongest echo. This non-adaptive approach is quite inefficient as it causes unnecessary processing loss for weak targets. For strong targets this processing loss has negligible impact on their detectability. However it may lead to missed detection of weak targets, especially those with SNRs near the detection threshold. This motivates the need to develop range sidelobe suppression techniques that minimise the processing loss for weak targets to improve detection sensitivity of the radar systems.

A number of adaptive pulse compression techniques have been reported in the literature. In [5], an adaptive technique based on reiterative minimum mean square error (MMSE) was introduced. It adaptively estimates an MMSE filter, which matches to the received signal, for each individual range cell. Extensions and applications of this approach can be found in [6]-[8]. A drawback of these techniques is that they require at least one matrix inversion of a structured covariance matrix for each MMSE filter. This can become problematic for radar waveforms with high-time bandwidth product, and may limit practical implementation in many real-time systems. Dimensionality reduction techniques based on splitting the full dimension covariance matrix into multiple lower dimension matrices were proposed in [9]. Despite efficient implementation of such dimensionality reduction, the computational complexity of these techniques still varies between 15 to 100 times greater than the MF.

Related work that addresses, in a different way, the issue of detecting weak targets in the presence of other strong echoes can be found in [10]-[16]. In [10]-[12], techniques based on extrapolating the waveform bandwidth and then applying a non-adaptive window over the extrapolated spectral region were proposed. These techniques result in range resolution and SNR improvements. However, they increase the data volume and require estimation of a set of auto-regressive (AR) models. The techniques in [13]-[16] are based on the principle of the CLEAN algorithm where the strong echoes are iteratively estimated and subtracted from the received signal to enable the detection of weak targets. These techniques

perform well for discrete-point targets but fail in cases of contiguous scattering sources. An extension of the CLEAN algorithm for contiguous scattering sources was discussed in [17]. This algorithm gives much better performance than the conventional CLEAN algorithm, but at the expense of significant complexity increase.

In this paper we propose a new technique to adaptively shape the spectral response of target returns, thereby controlling their range sidelobes adaptively. The novelty of this method involves applying the spectral shaping step after matched filtering and Doppler processing. This approach allows the target spectral responses to be separated into groups, each having a similar Doppler shift. Different spectral windows are then applied to different groups separately. The PSR of the window applied to a group is dependent on the strongest target signal within the group. As a result, a group containing low SNR targets requires a less severely tapered window than one with high SNR targets. This in turn leads to smaller processing loss, hence improving detection sensitivity of the radar systems. A practical attractiveness of the proposed adaptive technique is its low complexity. The total number of arithmetic operations carried out by the proposed technique is less than twice the number of operations required by the conventional non-adaptive technique.

## II. Preliminary

### A. Signal Model

We consider a radar system employing LFM waveforms. The continuous-time model of the transmitted waveform can be written as

$$s_t(t) = \sum_{p=0}^{P-1} s(t - pT) \ , \tag{1}$$

where

$$s(t) = \begin{cases} e^{j\pi\left(\alpha t^2 - Bt\right)} & 0 \le t \le T_o \\ 0 & \text{otherwise} \end{cases} \tag{2}$$

is the complex envelop of a single LFM pulse at baseband, $P$ is the number of pulses and $T$ is the pulse period. Here, $\alpha = B/T_o$ is the sweep rate measured in Hertz per second, $B$ is the waveform bandwidth and $T_o \le T$ is the pulse width. The instantaneous frequency of this baseband signal goes from $-\frac{B}{2}$ at $t = 0$ to $\frac{B}{2}$ at $t = T_o$. The signal $s(t)$ is referred to as a pulsed LFM signal when $T_o < T$ and as a linear frequency modulated continuous waveform (LFMCW) when $T_o = T$ [18].

The returned signal from $K$ targets and $N_c$ clutter-scatterers after it has been demodulated to baseband can then be modeled as

$$r(t) = \sum_{k=1}^{K} \sum_{\ell=1}^{L_k} \sum_{p=0}^{P-1} x_{k,\ell,p}(t) + \sum_{i=1}^{N_c} \sum_{\ell=1}^{L_i} \sum_{p=0}^{P-1} c_{i,\ell,p}(t) + v(t) \ , \tag{3}$$

where $x_{k,\ell,p}(t)$ corresponds to the target return of the $p^{th}$ pulse from the $k^{th}$ target via its $\ell^{th}$ propagation path, $c_{i,\ell,p}(t)$ corresponds to the clutter return of the $p^{th}$ pulse from the $i^{th}$ clutter-scatterer via its $\ell^{th}$ propagation path and $v(t)$ represents noise, which can be composed of internal receiver noise and external interferences. Note that in some radar environments the clutter distribution may be a continuum. The target return $x_{k,\ell,p}(t)$ and the clutter return $c_{i,\ell,p}(t)$ can be written as

$$x_{k,\ell,p}(t) = \alpha_{k,\ell} s(t - pT - \tau_{k,\ell})\, e^{j2\pi f_{k,\ell}(t-\tau_{k,\ell})} \tag{4}$$

$$c_{i,\ell,p}(t) = \beta_{i,\ell} s(t - pT - \tau_{i,\ell}) e^{j2\pi f_{i,\ell}(t-\tau_{i,\ell})} \ , \tag{5}$$

where $\alpha_{k,\ell}$, $\tau_{k,\ell}$ and $f_{k,\ell}$ respectively represent signal amplitude, time delay and Doppler shift of the $\ell^{th}$ path of the $k^{th}$ target and $\beta_{i,\ell}$, $\tau_{i,\ell}$ and $f_{i,\ell}$ represent amplitude, time delay and Doppler shift of the $\ell^{th}$ path of the $i^{th}$ scatterer.

### B. Conventional non-adaptive spectral shaping

The standard pulse compression technique correlates the received signal with a reference waveform $h(t)$. The output of the pulse compression process is given by

$$y(\tau) \triangleq \int_{-\infty}^{\infty} r(t) h(\tau - t) dt \ . \tag{6}$$

When the reference waveform is set to $h(t) = h_M(t) \triangleq s^*(T_M - t)$, it is known as a matched filter (MF). The constant $T_M \ge T_0$ is a delay constant required to make the filter physically realizable. It is well-known that the MF maximises the output SNR for a point scatterer in white Gaussian noise. However, it has a low PSR of around 13 dB. Consequently, weak targets can be masked by the range sidelobes of a stronger echo. To enhance the PSR and thereby allowing the detection of weak targets in the presence of stronger echoes, a spectral window $W(\omega)$ is often used to shape the spectral response of the reference waveform. This leads to a mismatched filter with the resulting reference waveform $h(t)$ now being given by

$$h(t) = \mathcal{F}^{-1}\{W(\omega) S^*(\omega) e^{-j\omega T_M}\} \ , \tag{7}$$

where $\mathcal{F}^{-1}$ denotes the inverse Fourier transform operation and $S(\omega)$ is the Fourier transform of $s(t)$.

## III. Adaptive Spectral Shaping

As discussed in Section I, the conventional non-adaptive technique needs to use a window with a PSR that exceeds the SNR of the strongest echo in the received signal. This is quite unattractive as it causes unnecessary processing loss for weak targets. This motivates us to develop a technique that adapts to the target strength. The idea here is to separate the target spectral responses into groups, each having a similar Doppler shift, and apply a spectral window with a PSR dependent on the strength of the strongest target in the group. This way the processing loss can be reduced for weak targets.

To see how different spectral windows can be separately applied to different groups of targets, we begin by deriving the spectral response of the pulse compression output when the reference signal $h(t)$ is set to the MF. The spectral response

the MF output can be computed directly from the Fourier transform of $h_M(t)$ and $r(t)$ as

$$Y_M(\omega) = H_M(\omega)\, R(\omega) \ . \tag{8}$$

The Fourier transform of $h_M(t)$ is given by

$$H_M(\omega) = S^*(\omega) e^{-j\omega T_M} \ . \tag{9}$$

By substituting (4) and (5) into (3), the Fourier transform of received signal $r(t)$ can be shown to be given by

$$R(\omega) = \sum_{k=1}^{K}\sum_{\ell=1}^{L_k}\sum_{p=0}^{P-1} X_{k,\ell,p}(\omega) + \sum_{i=1}^{N_c}\sum_{\ell=1}^{L_i}\sum_{p=0}^{P-1} C_{i,\ell,p}(\omega) + V(\omega) \tag{10}$$

where $V(\omega)$ is the Fourier transform of $v(t)$ and

$$X_{k,\ell,p}(\omega) = \alpha_{k,\ell} e^{j2\pi f_{k,\ell} pT} S\left(\omega - 2\pi f_{k,\ell}\right) e^{-j(pT+\tau_{k,\ell})\omega} \tag{11}$$

$$C_{i,\ell,p}(\omega) = \beta_{i,\ell} e^{j2\pi f_{i,\ell} pT} S\left(\omega - 2\pi f_{k,\ell}\right) e^{-j(pT+\tau_{i,\ell})\omega} \ . \tag{12}$$

The frequency response of the MF output can be expressed as a summation of individual target and clutter spectral responses

$$\begin{aligned} Y_M(\omega) = &\sum_{k=1}^{K}\sum_{\ell=1}^{L_k}\sum_{p=0}^{P-1} T_{k,\ell,p}(\omega) + \sum_{i=1}^{N_c}\sum_{\ell=1}^{L_i}\sum_{p=0}^{P-1} C_{i,\ell,p}(\omega) \\ &+ N(\omega) e^{-j\omega T_M} \ , \end{aligned} \tag{13}$$

where $N(\omega) = S^*(\omega)V(\omega)$, and $T_{k,\ell,p}(\omega)$ and $C_{i,\ell,p}(\omega)$ respectively correspond to the spectral response of the return signal of the $p^{th}$ pulse from the $k^{th}$ target and from the $i^{th}$ clutter scatterer via the $\ell^{th}$ propagation path. These two terms are given by

$$T_{k,\ell,p}(\omega) = \alpha_{k,\ell} e^{j2\pi f_{k,\ell} pT} Z(\omega, f_{k,\ell}) e^{-j(T_M+pT+\tau_{k,\ell})\omega} \tag{14}$$

$$C_{i,\ell,p}(\omega) = \beta_{i,\ell} e^{j2\pi f_{i,\ell} pT} Z(\omega, f_{i,\ell}) e^{-j(T_M+pT+\tau_{i,\ell})\omega} \tag{15}$$

with

$$Z(\omega, f_d) = S^*(\omega) S\left(\omega - 2\pi f_d\right) \ . \tag{16}$$

The MF output can be obtained from its spectral response $Y_M(\omega)$ by applying an inverse Fourier transform to it. This can be expressed as

$$\begin{aligned} y(\tau) = &\sum_{k=1}^{K}\sum_{\ell=1}^{L_k}\sum_{p=0}^{P-1} \alpha_{k,\ell} e^{j2\pi f_{k,\ell} pT} z(\tau - T_M - pT - \tau_{k,\ell}, f_{k,\ell}) \\ &+ \sum_{i=1}^{N_c}\sum_{\ell=1}^{L_i}\sum_{p=0}^{P-1} \beta_{i,\ell} e^{j2\pi f_{i,\ell} pT} z(\tau - T_M - pT - \tau_{i,\ell}, f_{i,\ell}) \\ &+ n(\tau - T_M) \ , \end{aligned} \tag{17}$$

where

$$z(\tau, f_d) = \mathcal{F}^{-1}\{Z(\omega, f_d)\} \tag{18}$$

and

$$n(\tau) = \mathcal{F}^{-1}\{N(\omega)\} \ . \tag{19}$$

The MF output can be partitioned into pulses according to

$$\begin{aligned} y_p(\bar{\tau}) &\triangleq y(\bar{\tau} + pT + T_M) \qquad (20) \\ &= \sum_{k=1}^{K}\sum_{\ell=1}^{L_k} \alpha_{k,\ell} e^{j2\pi f_{k,\ell} pT} \lambda(\bar{\tau}, f_{k,\ell}, \tau_{k,\ell}) \\ &+ \sum_{i=1}^{N_c}\sum_{\ell=1}^{L_i} \beta_{i,\ell} e^{j2\pi f_{i,\ell} pT} \lambda(\bar{\tau}, f_{i,\ell}, \tau_{i,\ell}) \\ &+ n(\bar{\tau} + pT + T_M) \ , \qquad (21) \end{aligned}$$

where $0 \le \bar{\tau} \le T$ and $\lambda(\bar{\tau}, f_d, \tau_d)$ is the point spread function of a target or scatterer with a Doppler shift $f_d$ and a time delay $\tau_d$

$$\lambda(\bar{\tau}, f_d, \tau_d) = \sum_{q=-1}^{1} e^{j2\pi f_d qT} z\left(\bar{\tau} - qT - \tau_d, f_d\right) \ . \tag{22}$$

From (21), the MF output corresponding to a target or clutter return varies from pulse to pulse according to a sinusoid. By applying Doppler processing across the pulses, we now have a range profile at the Doppler bin $f_b$

$$\mathcal{Y}_M(\bar{\tau}, f_b) \triangleq \sum_{p=0}^{P-1} w_p y_p(\bar{\tau}) e^{-j2\pi pT f_b} \ , \tag{23}$$

where $W_t = [w_0 \ w_1 \ \ldots \ w_{P-1}]$ is a temporal window that controls the Doppler sidelobes and $f_b$ is the frequency of a Doppler bin of interest. By substituting (21) into (23), the Fourier transform of the range profile $\mathcal{Y}_M(\bar{\tau}, f_b)$ at the Doppler bin $f_b$ can be expressed as

$$\begin{aligned} Y_M(\omega, f_b) &\triangleq \mathcal{F}\left\{\mathcal{Y}_M(\bar{\tau}, f_b)\right\} \qquad (24) \\ &= \sum_{k=1}^{K}\sum_{\ell=1}^{L_k} \alpha_{k,\ell} \varphi(f_b, f_{k,\ell}) \Lambda(\omega, f_{k,\ell}, \tau_{k,\ell}) e^{-j\tau_{k,\ell}\omega} \\ &+ \sum_{i=1}^{N_c}\sum_{\ell=1}^{L_i} \beta_{i,\ell} \varphi(f_b, f_{i,\ell}) \Lambda(\omega, f_{i,\ell}, \tau_{i,\ell}) e^{-j\tau_{i,\ell}\omega} \\ &+ \sum_{p=0}^{P-1} w_p e^{-j2\pi pT f_b} N(\omega) e^{jpT\omega} \ , \qquad (25) \end{aligned}$$

where

$$\varphi(f_b, f_d) = \sum_{p=0}^{P-1} w_p e^{j2\pi(f_{k,\ell} - f_b)pT} \tag{26}$$

and

$$\Lambda(\omega, f_d, \tau_d) = \mathcal{F}\{\lambda\left(\text{mod}(\bar{\tau} + \tau_d, T), f_d, \tau_d\right)\} \tag{27}$$

with $\text{mod}(\cdot,\cdot)$ denotes the modulo operation.

The resulting $Y_M(\omega, f_b)$ is the spectral response of the range profile at the Doppler shift $f_b$. It still contains the spectral responses of all targets and clutter-scatterers. However, the contribution from a target or clutter-scatterer to the spectrum $Y_M(\omega, f_b)$ is determined by the temporal weighting function $W_t$. For targets or clutter-scatterers that are not close to the Doppler shift $f_b$, their contribution to the spectrum $Y_M(\omega, f_b)$ would be negligible. Hence, the steps of Doppler processing

the MF output to produce $\mathcal{Y}_M(\bar{\tau}, f_b)$ and Fourier transforming it to $Y_M(\omega, f_b)$ have effectively separated the target and clutter-scatterer spectral responses into groups, each having a similar Doppler shift.

With the above separation of the spectral responses, we can now apply different windows to different Doppler bins. The PSR of the window applied to a group will be adjusted according to the strength of the strongest return within the group. In this paper, we employ a Taylor window for each group with its PSR adjusted adaptively. Let $W_{a,f_b}(\omega)$ denotes the window being applied to spectrally shape the response $Y_M(\omega, f_b)$. The final range profile at the Doppler shift $f_b$ after adaptive spectral shaping will now be given by

$$\mathcal{Y}_{adapt}(\bar{\tau}, f_b) \triangleq \mathcal{F}^{-1}\left\{W_{a,f_b}(\omega)\ Y_M(\omega, f_b)\right\}\ . \qquad (28)$$

## IV. Performance Assessment

The performance of the proposed adaptive spectral shaping technique is assessed using both simulated and real data. In both cases, we consider a skywave over-the-horizon (OTH) radar system where it exploits refraction of electromagnetic waves by the ionosphere to detect and track targets well beyond the horizon. We compare the performance of the proposed adaptive technique with that of the conventional non-adaptive spectral shaping technique. We will not compare with other adaptive range sidelobe suppression techniques such as those presented in [9] and [17] as their complexities are significantly greater than our proposed method. As will be shown subsequently, the proposed adaptive method gains back almost all the SNR loss incurred by the non-adaptive method for weak targets at the cost of less than doubling the computational complexity.

### A. Simulated Results

We use an LFMCW signal which consists of $P = 64$ pulses (also known as sweeps) with a bandwidth of 10 kHz and a repetition frequency of 50 Hz. We assume a clutter environment with additive white Gaussian noise. The clutter return is assumed to be composed of ground echoes which have zero Doppler shifts with an average input clutter-to-noise ratio (CNR) of 60 dB. The electromagnetic waves are assumed to be refracted from a single layer in the ionosphere (i.e. $L_k = 1$ for all $k$ and $L_i = 1$ for all $i$). We insert into the received signal five targets at various ranges. The input SNR, range and Doppler shift of these targets are summarised in Table I. The input CNR and input SNR are respectively defined as $N|\beta_{i,1}|^2/\sigma^2$ and $N|\alpha_{k,1}|^2/\sigma^2$ where $N$ is the number of samples of the received signal during the $P$ pulses and $\sigma^2$ is the noise power. The received signal is sampled at the sampling rate $f_s = 32.5$ kHz.

In this simulated scenario a Taylor window with a PSR of 80 dB is used as the temporal window (i.e. $W_t$) to suppress the Doppler sidelobes in the Doppler processing step. To achieve range sidelobe suppression by the non-adaptive technique a Taylor window with a PSR of 60 dB is used as the spectral window (i.e. $W_{max}(\omega)$). The theoretical processing loss for the non-adaptive technique associated with this window is 1.9 dB.

TABLE I
Simulated targets' signal strength, range and Doppler shift

| Target | Doppler shift (Hz) | Input SNR (dB) | Range (km) |
|---|---|---|---|
| 1 | -18 | 22 | 1477 |
| 2 | 10 | 50 | 1215 |
| 3 | 10 | 30 | 1286 |
| 4 | 15 | 15 | 1513 |
| 5 | 20 | 35 | 1374 |

TABLE II
Targets' Output SNR

| Target | Non-adaptive | Adaptive | Gain (dB) |
|---|---|---|---|
| 1 | 19.2 | 20.8 | 1.6 |
| 2 | 44.1 | 44.5 | 0.4 |
| 3 | 24.1 | 24.5 | 0.4 |
| 4 | 12.3 | 14.0 | 1.7 |
| 5 | 31.4 | 32.3 | 0.9 |

For the proposed adaptive technique Taylor windows are also used, but with their PSR being set adaptively on a Doppler bin by bin basis. Fig. 1 and 2 respectively show the range-Doppler intensity maps produced by the conventional non-adaptive technique and the proposed adaptive technique for one noise realisation. The intensity level is colour coded with the JET colormap with its strongest intensity represented by dark red and weakest intensity represented by dark blue. Fig. 3 shows cuts along the range dimension at Doppler bins containing the targets. In these results the range profile at each Doppler bin has been normalised so that the average background noise is at 0 dB. Thus, the magnitudes given in Fig. 3 correspond to the output SNR of each target. Table II summarises the average output SNR and the associated SNR gains for all five targets. These values were obtained by averaging over 1000 different noise realisations. As expected, the proposed adaptive technique produces higher output SNR than the conventional non-adaptive technique. The relative gain are higher for targets in Doppler bins that have only weak targets than those in Doppler bins containing a strong target. For example, the proposed method achieves an SNR gain of 1.7 dB for Target 4 in Doppler bin $f_b = 15$ Hz while only 0.4 dB for Target 2 in Doppler bin $f_b = 10$ Hz. With an SNR gain of 1.7 dB for Target 4 this implies that the proposed adaptive technique has reduced a processing loss of 1.9 dB, as incurred by the non-adaptive method, down to only 0.2 dB. It should be noted that a processing loss of few dBs has negligible impact on the detectability of strong targets but will have a severe impact on the detectability of weak targets. Consequently, it is of more importance to reduce the processing loss for weak targets than strong targets. In addition to reducing the processing loss, the adaptive technique improves target range resolution. This is evident by a smaller target mainlobe width in the range profiles produced by the adaptive technique.

### B. Experimental Results

In addition to simulation, we have also used real data from an OTH radar of the Jindalee Operational Radar Network (JORN) to evaluate the performance of the proposed technique.

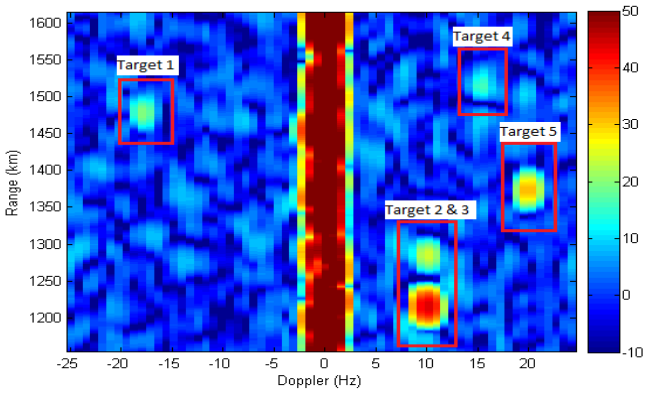


Fig. 1. Simulated data: Range-Doppler map produced with non-adaptive spectral shaping

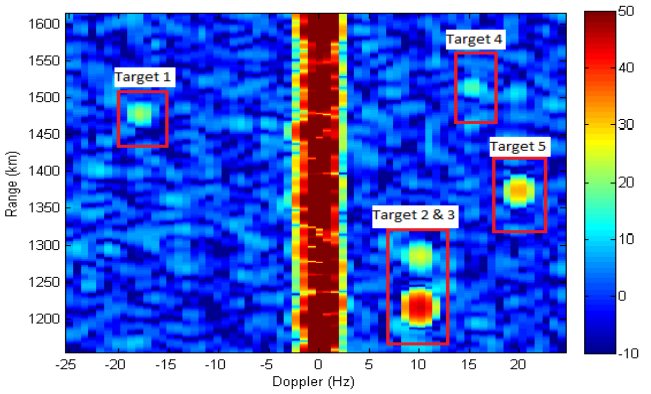


Fig. 2. Simulated data: Range-Doppler map produced with adaptive spectral shaping

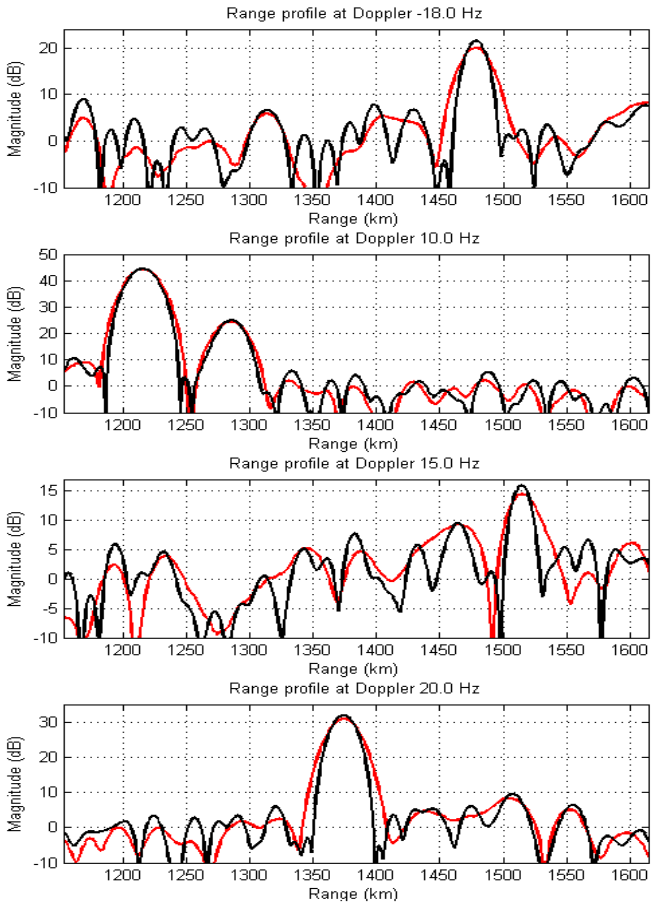


Fig. 3. Simulated data: Comparison of range profile at various Doppler bin. Range profiles produced by non-adaptive spectral shaping are plotted in red and by adaptive spectral shaping are plotted in black

This OTH radar system is situated in Laverton, Western Australia. An LFMCW waveform was transmitted by a linear antenna array of 28 elements and the returned signals were collected by a 3 km linear antenna array of 480 elements. The received signals were digitised and beamformed using a conventional beamformer. The signal from a beam of interest was then used to assess the performance.

Fig. 4 and 5 respectively show the range-Doppler intensity maps produced by the conventional non-adaptive technique and the adaptive technique for the beam of interest. There are four targets clearly present in this beam with each arriving at the receiver through multiple paths and at different Doppler shift. Fig. 6 compares the range profiles of the four targets. These range profiles have been normalised so that the average background noise is at 0 dB. Similar to the simulated results, these comparisons demonstrate gains in terms of output SNR and resolution improvements by the proposed adaptive technique over the non-adaptive technique. The SNR improvement is more significant for weaker targets with the weakest Target 4 having a gain of around 1.6 dB.

## V. Conclusions

We have proposed a new method to reduce processing loss of pulse compression methods that adopt spectral shaping to achieve range sidelobe suppression. The novelty of the proposed technique involves applying the spectral shaping after the matched filtering and Doppler processing steps. This allows the target spectral responses to be separated into groups, each having a similar Doppler shift. Different windows are then applied to different groups separately. The PSR of the window applied to a group is dependent on the strongest target signal within the group. As a result, a group containing low SNR targets requires a less severe window than one with high SNR targets. This in turn leads to smaller processing loss. A practical attractiveness of the proposed adaptive technique is its low complexity. The total number of arithmetic operations carried out by the proposed technique is less than twice the number of operations required by the conventional non-adaptive technique. We have verified the performance gain of the proposed adaptive technique over the non-adaptive technique using both simulated and real data.

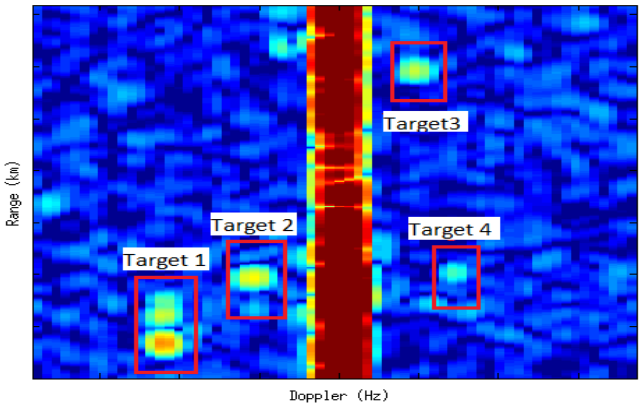


Fig. 4. Real data: Range-Doppler map produced with non-adaptive spectral shaping

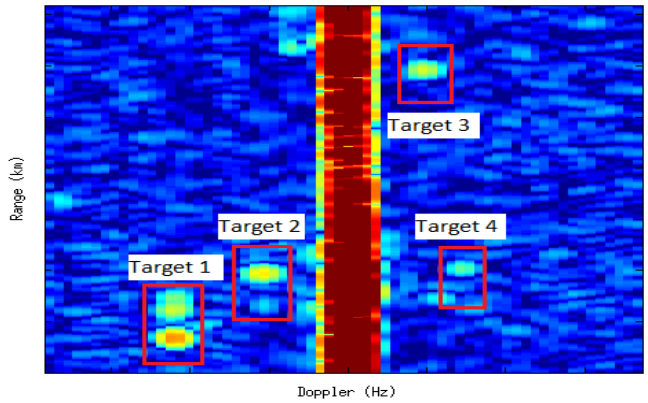


Fig. 5. Real data: Range-Doppler map produced with adaptive spectral shaping

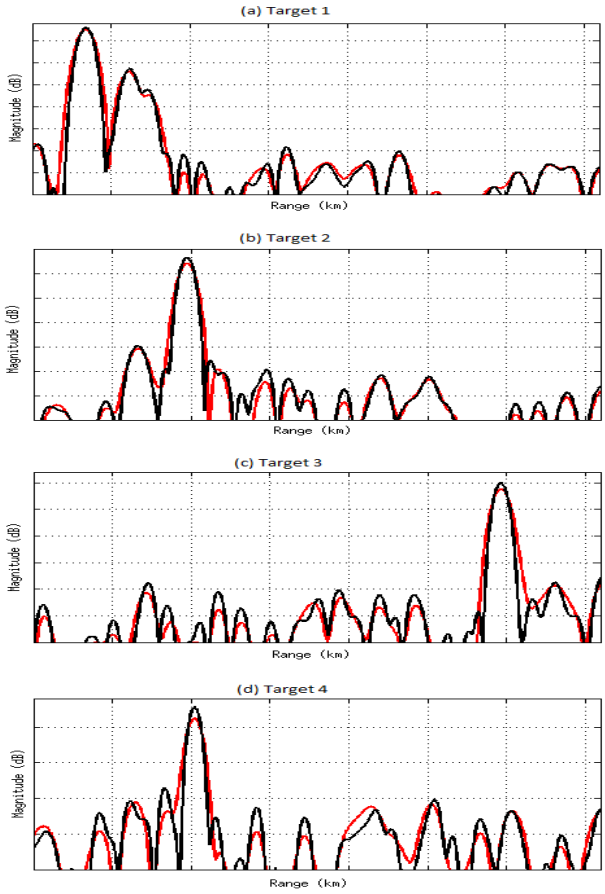


Fig. 6. Real data: Comparison of range profile at various Doppler bin. Range profiles produced by non-adaptive spectral shaping are plotted in red and by adaptive spectral shaping are plotted in black

## REFERENCES


[1] M. I. Skolnik, *Introduction to Radar Systems*. Kogakusha, Japan: McGraw-Hill, 1981.

[2] L. R. Varshney and D. Thomas, "Sidelobe reduction for matched filter range processing," *IEEE Radar Conference*, Huntsville, AL, USA, 5-8 May, 2003, pp. 446-451.

[3] M. A. Richard, *Fundamentals of Radar Signal Processing*, New York: McGraw-Hill, 2005.

[4] F. J. Harris, "On the use of windows for harmonic analysis with the discrete Fourier transform," *Proceedings of IEEE*, vol. 66, pp. 51-83, Jan. 1978.

[5] S. D. Blunt and K. Gerlach, "Adaptive pulse compression via MMSE estimation," *IEEE Trans. Aerospace and Electronic Systems*, vol. 42, pp. 572-584, Apr. 2006.

[6] K. Gerlach and S. D. Blunt, "Radar pulse compression repair," *IEEE Trans. Aerospace and Electronic Systems*, vol. 43, pp. 1188-1195, Apr. 2007.

[7] S. D. Blunt, A. K. Shackelford, K. Gerlach and K. J. Smith, "Doppler compensation & single pulse imaging using adaptive pulse compression," *IEEE Trans. Aerospace and Electronic Systems*, vol. 45, pp. 647-659, Apr. 2009.

[8] T. Higgins, S. D. Blunt and K. Gerlach, "Gain-constrained adaptive pulse compression via an MVDR framework," *IEEE Radar Conference*, Pasadena, CA, USA, 4-8 May, 2009.

[9] S. D. Blunt and T. Higgins, "Dimensionality reduction techniques for efficient adaptive pulse compression," *IEEE Trans. Aerospace and Electronic Systems*, vol. 46, pp. 349-362, Jan. 2010.

[10] Cuomo, K. M. "A bandwidth extrapolation technique for improved range resolution of coherent radar data," *MIT Lincoln Laboratory Project Report CPJ-60*, Rev. 1, DTIC ADA-258462, Dec. 1992.

[11] V. K. Nguyen and M. D. Turley, "Bandwidth extrapolation of LFM signals for narrowband radar systems," *International Conference on Radar*, Adelaide, Australia, pp. 140-145, 9-12 Sept. 2013.

[12] V. K. Nguyen and M. D. E. Turley, "Bandwidth extrapolation of LFM signals for narrowband radar systems," *IEEE Trans. Aerospace and Electronic Systems*, vol. 51, pp. 702-711, Jan. 2015.

[13] Y. I. Abramovich,"Compensation methods for the resolution of wide-band signals, *Radio Eng. Elect. Phys.*, vol. 23, pp. 5459, Jan. 1978.

[14] A. Segalovitz and B. R. Frieden, "A CLEAN-type deconvolution algorithm, *Astron. Astrophys.*, vol. 70, pp. 335343, 1978.

[15] B. G. Clark, "An efficient implementation of the algorithm CLEAN, Astron. Astrophys., vol. 89, pp. 377378, 1980.

[16] J. Tsao and B. Steinberg, "Reduction of sidelobe and speckle artifacts in microwave imaging: The CLEAN technique, *IEEE Trans. Antenna Propagat.*, vol. 36, pp. 543556, Apr. 1988.

[17] R. Bose, A. Freedman and B. D. Steinberg, "Sequence CLEAN: a modified deconvolution technique for microwave images of contiguous targets", *IEEE Trans. Aerospace and Electronic Systems*, vol. 38, pp. 89-97, Jan. 2002.

[18] V. K. Nguyen, "A low complexity parameter estimation technique for LFMCW signals," *IEEE Trans. Aerospace and Electronic Systems*, vol. 50, pp. 2554-2563, Oct. 2014.